BILINGUAL PUBLISHING GROUP

Journal of Electronic & Information Systems

https://journals.bilpubgroup.com/index.php/jeis

ARTICLE

Evaluating Maximum Diameters of Tumor Sub-regions for Survival Prediction in Glioblastoma Patients via Machine Learning, Considering Resection Status

***R Babaei*[1], *A Bonakdar*[1], *N Shakourifar*[1], *M Soltani*[1,2,3,4,7*], *K Raahemifar*[5,6,7]**

[1] *Department of Mechanical Engineering, K. N. Toosi University of Technology, Tehran, 15418-49611, Iran*
[2] *Department of Electrical and Computer Engineering, University of Waterloo, Waterloo, Ontario, N2L 3G1, Canada*
[3] *Centre for Biotechnology and Bioengineering (CBB), University of Waterloo, Waterloo, Ontario, N2L 3G1, Canada*
[4] *Advanced Bioengineering Initiative Center, Computational Medicine Center, K. N. Toosi University of Technology, Tehran, 15418-49611, Iran*
[5] *College of Information Sciences and Technology (IST), Data Science and Artificial Intelligence Program, Penn State University, State College, Pennsylvania, PA, 16801, United States of America*
[6] *Chemical Engineering Department, University of Waterloo, Waterloo, ON, N2L 3G1, Canada*
[7] *Optometry & Vision Science Department, University of Waterloo, Waterloo, ON, N2L 3G1, Canada*

ABSTRACT

In recent decades, there have been significant advancements in medical diagnosis and treatment techniques. However, there is still much progress to be made in effectively managing a wide range of diseases, particularly cancer. Timely diagnosis of cancer remains a critical step towards successful treatment, as it significantly impacts patients' chances of survival. Among various types of cancer, glioma stands out as the most common primary brain tumor, exhibiting different levels of aggressiveness. One of the monitoring techniques is magnetic resonance imaging (MRI) which provides a precise visual representation of the tumor and its sub-regions (edema (ED), enhancing tumor (ET), and non-enhancing necrotic tumor core (NEC)), enabling monitoring of its location, shape, and sub-regional characteristics. In this study, the authors aim to investigate the underlying relationship between the maximum diameters of tumor sub-regions and patients' overall survival (OS) in glioblastoma cases. Using an MRI dataset of glioblastoma patients, the authors categorized them based on resection status: gross total resection (GTR) and unknown (NA). By employing the Euclidean distance algorithm, the authors estimated the sub-regions' maximum diameters. Machine learning algorithms were used to explore the correlation between sub-regions' maximum diameters and survival outcomes. The results of the univariate prediction models showed that tumor sub-regions' maximum diameters have a noticeable correlation with the survival rates among patients with unknown resection status with the average Spearman correlation of –0.254. Also, the addition of the sub-regions' maximum diameter feature to the radiomics increased the accuracy of ML algorithms in predicting the survival rates with an average of 4.58%.

Keywords: Machine learning; Radiomics; Glioblastoma; Tumor sub-regions; BraTS 2019

*CORRESPONDING AUTHOR:
M Soltani, Department of Mechanical Engineering, K. N. Toosi University of Technology, Tehran, 15418-49611, Iran; Department of Electrical and Computer Engineering, University of Waterloo, Waterloo, Ontario, N2L 3G1, Canada; Centre for Biotechnology and Bioengineering (CBB), University of Waterloo, Waterloo, Ontario, N2L 3G1, Canada; Advanced Bioengineering Initiative Center, Computational Medicine Center, K. N. Toosi University of Technology, Tehran, 15418-49611, Iran; Optometry & Vision Science Department, University of Waterloo, Waterloo, ON, N2L 3G1, Canada; Email: msoltani@uwaterloo.ca

ARTICLE INFO
Received: 23 December 2023 | Revised: 18 January 2023 | Accepted: 28 February 2024 | Published Online: 22 March 2024
DOI: https://doi.org/10.30564/jeis.v6i1.6174

CITATION
Babaei, R., Bonakdar, A., Shakourifar, N., et al., 2024. Evaluating Maximum Diameters of Tumor Sub-regions for Survival Prediction in Glioblastoma Patients via Machine Learning, Considering Resection Status. Journal of Electronic & Information Systems. 6(1): 22–38. DOI: https://doi.org/10.30564/jeis.v6i1.6174

1. Introduction

According to WHO reports, cancer is the second cause of death in the world. Cancers have various ranges of aggressiveness. Some are more treatable and can be diagnosed early, while others have higher fatality due to their late symptoms' indications and inadequate response to drugs [1]. The majority of brain tumor patients are those with glioma, which is an intra-axial tumor. Glioma includes almost 30% of all brain tumors beginning in glial cells [2,3]. Based on the cancer aggressiveness, glioma can be subdivided into low-grade glioma (grade I and II) and high-grade glioma (grade III and IV). Among all types of glioma, glioblastoma (GBM) is less treatable, and only 5% of patients diagnosed with GBM have a 5-year survival chance [4]. One of the main difficulties in the therapeutic intervention of GBM is the complex structure of the tumor. It is multiform microscopically, with various regions including pseudopalisading necrosis, pleomorphic nuclei and cells, and microvascular proliferation [5].

Numerous ways have been investigated to estimate the malignancy of tumors and patients' cancer status to predict better further clinical strategies and the chance of surviving. TNM staging is an acceptable way that classifies tumors based on three main criteria: primary brain tumor (T), regional lymph nodes (N), and distance metastasis (M). Besides, some studies have investigated the effect of social [6], physical [7], and economic features [8] on patients' OS. Additionally, the utilization of general features like age and gender as standalone factors for predicting overall survival (OS) in patients has yielded discouraging results [9], mainly due to their lack of individualization [10]. Although medical images contain lots of information that can be detected by the naked eye, numerous quantitative features can be extracted from images by computer-aided algorithms that can describe the disease aggressiveness more accurately [11]. Indeed, automatic analysis of images would be a respectful replacement for traditional approaches and provides more precise results [12].

Radiomics is an emerging method that extracts a large number of quantitative medical imaging features capable of advanced image-based tumor phenotyping, providing valuable clinical information for OS prediction [13]. Early radiomics approaches were the semantic analysis as the radiologists tried to figure out the images only qualitatively. Following the rapid developments of computer-aided algorithms, the field moved quickly toward high-throughput analyses, which led to the extraction of quantitative features from images [14]. More importantly, these features have shown excellent potential to improve the prognostic of glioblastoma patients when integrated with conventional clinical and genetic prognostic models [12].

Hooper [15] reviewed various MRI radiomic features of glioblastoma, providing an overview of the potential applications of radiomics in this context. Zhu [16] developed a non-invasive prediction model for overall survival time in glioblastoma patients based on multimodal MRI radiomics, highlighting the potential of radiomic features in predicting patient outcomes. Furthermore, Li [17] proposed a multiparameter radiomic model for accurate prognostic prediction of glioma, demonstrating the development of novel prognostic radiomic models for predicting the prognosis of glioma.

In the field of glioma research, other studies have employed different approaches. Weninger [9] investigated an age-only regression model, achieving an accuracy of 56% and highlighting that the addition of radiomics to the age parameter did not necessarily improve prediction accuracy for different resection statuses. Shboul [18] utilized random forest regression (RFR) with radiomic features, while Feng [19] employed linear models with geometric features, achieving accuracies of 58% and 62% respectively [20]. Other studies have explored the use of deep models integrated with radiomics for gliomas [21], full-resolution residual convolutional neural networks (FRRN) [22], RFR with atlas locations and tumor's relative size using a "pseudo-3D" method [23], and RFR method [24]. Choi investigated the impact of radiomic features

on a random survival forest model, demonstrating a nearly 7% improvement in performance by incorporating radiomics [25]. Similarly, Wankhede [26] used a hybrid model integrating deep features from MRI using the convolutional neural network (CNN) and radiomic features extracted with modified fuzzy C-means (MFCM) clustering algorithm and achieved approximately 20% higher accuracy in glioblastoma survival prediction compared to conventional models. Hu [27] combined radiomics, deep features, and patient-specific clinical features that indicated higher prediction accuracy (0.745) compared to using age and tumor region volumes only (0.638).

The BraTS is a widely used dataset entailing multimodal MRI scans of glioblastoma patients. These scans include T1-weighted MRI (T1), T1-weighted MRI with contrast enhancement (T1CE), T2-weighted MRI (T2), and fluid-attenuated inversion recovery (FLAIR). T1-weighted images are widely utilized for analyzing brain tumor structures due to their ability to facilitate the annotation of healthy tissues [28]. In T1CE sequence images, the borders of brain tumors appear brighter as a result of contrast agent accumulation, allowing for easy differentiation of the necrotic core. Additionally, in T2-weighted images, the edema region appears brighter compared to other areas. The FLAIR scan is particularly useful in distinguishing the edema region from the cerebrospinal fluid (CSF). By combining these distinct MRI sequences, radiomic features can be extracted from the images [29].

In recent years, multimodal assessment has become increasingly popular for its enhanced performance and accuracy. It involves combining various factors such as demographic, socioeconomic, clinical, and radiographic features to predict OS more effectively [30]. However, the influence of tumor sub-regions' maximum diameters on this assessment has not been thoroughly examined.

This study aims to explore the influence of the maximum diameters of sub-regions (edema (ED), enhancing tumor (ET), and non-enhancing necrotic tumor core (NEC) in glioblastoma (GBM)) on the prediction of OS, in conjunction with radiomic features. The training dataset exclusively consists of reliable segmentations from the BraTS 2019 database provided by multiple experts following a consistent annotation protocol, and subsequently validated by experienced neuro-radiologists. To account for the impact of resection status, the dataset was divided into two groups: patients with gross total resection status (GTR) and those with unknown resection status (NA), enabling separate analysis. The maximum diameters of tumor sub-regions were extracted from MRI images, and the individual influence of each feature on OS was evaluated using different regression algorithms. Additionally, the automatic extraction of radiomic features was performed, followed by the elimination of redundant features and the selection of the most relevant ones using feature reduction algorithms. Ultimately, these selected features were then used independently in multivariate prediction models. Additionally, an investigation was conducted to determine if the addition of tumor sub-regions' maximum diameters to these features enhances the robustness of OS prediction.

In the "Materials" section, the article provides information on the dataset and details about the cohort study used in the research. The "Methods" section encompasses stages including image preprocessing, radiomic feature extraction, standardization, and preselection of radiomic features. It also covers the statistical hypothesis testing of preselected radiomic features, the procedure for tumor sub-regions' feature extraction, and the development of prediction models. The "Results" section outlines radiomic feature reduction outputs, hypothesis testing outcomes, as well as the results from univariate and multivariate prediction models. The "Discussion" section delves into the interpretation of findings and explores their implications. Lastly, the "Conclusions" section presents a summary of key findings, suggesting potential directions for future research.

2. Materials

The BraTS 2019 training dataset, a well-known

resource in the medical field has been used in this study. Its key elements, including four MRI acquisitions and a comprehensive segmentation map, are explored. Patient data, specifically survival days and resection status, is considered for the purpose of this study. Beyond the dataset, a comprehensive cohort analysis is included in the study to examine how prediction models are influenced by population variations and treatment choices.

2.1 Dataset

The BraTS challenge, which has been held annually since 2012, serves as a platform for comparing different segmentation algorithms. Starting in 2017, the challenge introduced quantitative image features to explore the potential enrichment of clinical insights and the improvement in predicting patients' OS [20,31–34].

In this study, we utilized the BraTS 2019 training dataset, which encompasses four MRI acquisitions (T1, T1CE, T2, and T2-FLAIR), along with a segmentation map that includes edema (ED), enhancing tumor (ET), and non-enhancing necrotic tumor core (NEC). Each of the sequences represents a specific part of the tumor brighter. A tumor segmentation map, which is necessary for radiomic feature extraction, is acquired by integrating all of the sequences.

Additionally, the dataset provides information on the survival days and resection status of 211 glioblastoma (GBM) patients, whose OS spans a range of 3 to 1767 days. Patients were divided into two groups based on the resection status: patients reported as GTR; and patients whose resection status is unavailable (NA).

The BraTS challenge has classified patients' OS into three categories: long-survivors (e.g., > 450 days), short-survivors (e.g., < 300 days), and mid-survivors (e.g., between 300 and 450 days). For the purpose of this study, 450 days were selected as the midpoint to create two distinct groups for classification purposes. However, when using regression models, the exact survival days were considered and fitted to the data.

2.2 Cohort study

The BraTS dataset primarily consists of data from the Center for Biomedical Image Computing and Analytics (CBICA) at the University of Pennsylvania and the Cancer Imaging Archive (TCIA). Although variations in population, imaging protocols, and treatment can have a noticeable impact on prediction models, certain parameters exhibit similarities within this dataset.

Initially, it is important to note that all patients with gross total resection (GTR) and unknown resection (NA) statuses are derived from the CBICA institution and TCIA, respectively. Consequently, there is no substantial disparity in the distribution of each dataset. Additionally, a significant statistical measure, known as the p-value, was employed to assess whether there were notable differences between the groups. Specifically, the p-value was obtained through a one-way analysis of variance. In this dataset, the calculated p-value exceeds 0.05, indicating the absence of significant statistical differences in terms of age or survival among the groups. To visually depict this similarity and facilitate comparison, **Figure 1** illustrates the age and survival day variations for both the GTR and NA groups.

3. Methods

This study employs a set of essential procedures outlined by Soltani [35]. These procedures encompass image preprocessing, radiomic feature extraction, and feature reduction. Additionally, we extracted the maximum diameters of tumor sub-regions and incorporated them into learning algorithms to evaluate their influence on patients' OS.

The significance of these steps is visually represented in **Figure 2**. In the following section, a more detailed explanation of each step is provided.

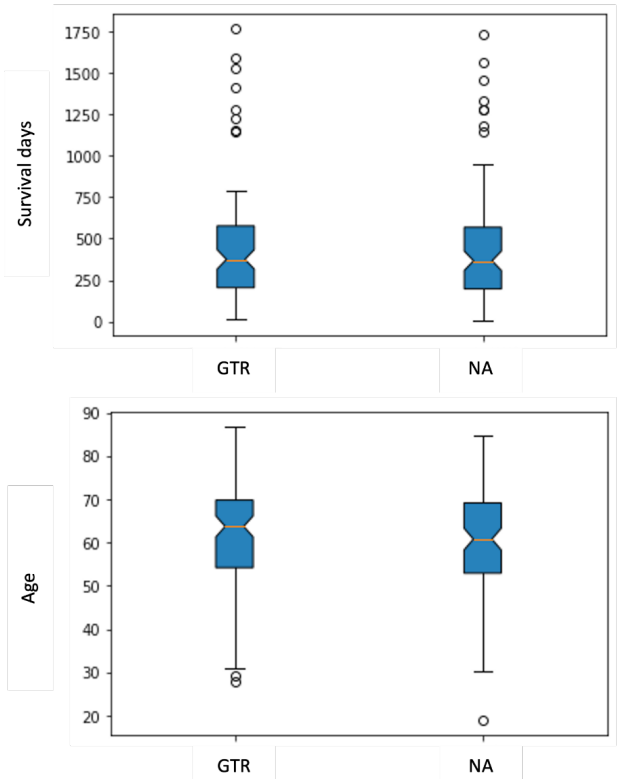

Figure 1. Distribution of age and survival days in patients with gross total resection status (GTR) and patients with unknown resection status (NA).

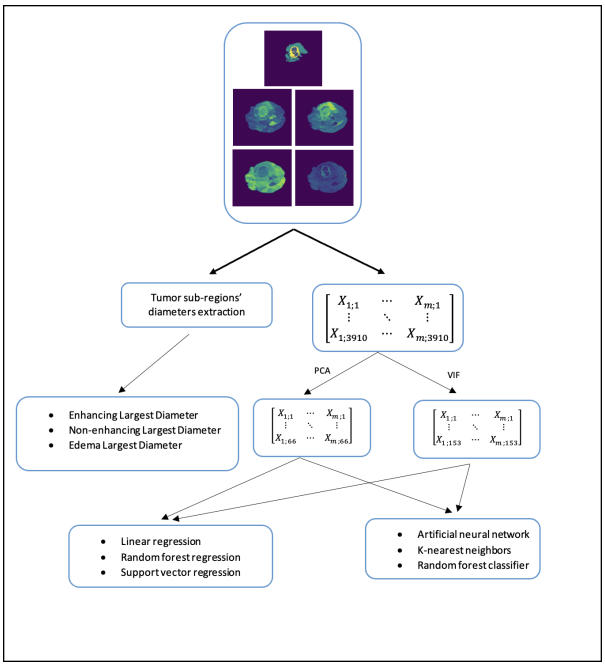

Figure 2. Methodology used to evaluate the predictiveness of location-based features independently and in combination with radiomics for overall survival.

3.1 Image preprocessing

Due to the limited dataset used in this study, it is necessary to normalize the images in order to reduce diversity and potential imaging errors. To achieve this, we followed the approach outlined in previous relevant studies and opted for N4 bias field correction and z-score normalization [36]. These techniques were employed to address differences in image intensities and ensure that the images are normalized in terms of both variance and zero mean.

- Z-score normalization: Z-score normalization, also known as standardization, is a technique used to normalize the pixel values of an image. It involves subtracting the mean value of the pixel intensities from each pixel and then dividing the result by the standard deviation of the pixel intensities. Mathematically, the z-score formula can be expressed as follows, where μ is the population mean, σ is the population standard deviation, and x is the individual data point being evaluated:

$$z = \frac{x - \mu}{\sigma}$$

z-score normalization

- N4 bias field correction: N4 bias field correction is a commonly used technique in medical image preprocessing. It involves employing a multi-scale optimization approach to estimate and correct for a smooth, slowly varying and multiplicative field present in the images. This correction helps address intensity variations caused by factors such as uneven illumination or magnetic field inhomogeneities. Gaillochet [37] demonstrated the effectiveness of N4 bias field correction in their research, supporting its usefulness as a preprocessing step in medical image analysis.

3.2 Radiomic feature extraction

To extract the radiomic features, we utilized the Pyradiomics module, as introduced by Griethuysen [38]. This module offers a comprehensive set of tools and algorithms specifically designed for radiomic feature extraction. The extracted features encompass various categories, including first-order statistics,

shape-based features (both 3D and 2D), gray level co-occurrence matrix, gray level run length matrix, gray level size zone matrix, neighboring gray-tone difference matrix, and gray level dependence matrix. These features provide valuable information about the texture, shape, and spatial relationships within the medical images, enabling a more comprehensive characterization of the tumor sub-regions.

A total of 3910 features were extracted from the images, while there was a total of 201 patients with GTR and NA resection status. In order to prevent overfitting and enhance the efficiency of the modeling process, feature reduction algorithms, as described by Bzdok [39], were applied. These algorithms helped in selecting the most important features, reducing the dimensionality of the dataset, and mitigating the risk of overfitting.

3.3 Standardization and preselection of features

To ensure reliable predictive models and address variability, the radiomic features were initially standardized using the scikit-learn object StandardScaler to have a value between zero and one. Reducing the dimensionality of the features became necessary due to redundancy. Therefore, the correlation matrix was first applied, followed by the variance inflation factor (VIF) and principal component analysis (PCA) independently.

- Correlation Matrix: In this approach, a simple linear regression was performed between each individual feature and the others. The pairwise correlations were evaluated, and representative features were selected based on their correlations [40]. In the correlation matrix, areas with correlations above 95 percent were reduced to retain the most variable element.
- Variance Inflation Factor (VIF): The VIF preselection method was applied to the remaining features after the correlation matrix step to address multicollinearity. The commonly recommended threshold is 10, and features exhibiting a VIF exceeding this value were removed to address concerns related to collinearity.
- Principal Component Analysis (PCA): PCA was employed to extract essential information from the dataset [41] and reduce dimensionality [42]. After applying PCA to the features outputted from the correlation matrix, only the features capturing 95 percent of the variance in the data were retained for the subsequent learning process.

3.4 Statistical hypothesis testing

To assess the impact of individual features on OS prediction and control for false discoveries, hypothesis tests were deemed necessary. It is important to note that controlling the false discovery rate (FDR) on PCA-selected features is not required, as this algorithm selects the most relevant elements based on their association with OS. On the other hand, VIF eliminates features based on multicollinearity, with OS having no influence on the VIF selection process. Hence, the Benjamini-Hochberg procedure [43] was applied to the data remaining after VIF feature selection, using a specific level of $\alpha = 0.05$, to control the FDR and minimize the risk of false discoveries.

3.5 Tumor sub-regions' feature extraction

The primary objective of this study is to assess the predictive value of tumor sub-regions' maximum diameters on overall survival (OS) in patients with different resection statuses as it provides valuable information about the extent and size of the tumor sub-regions, which has significant implications for treatment planning and patient prognosis. To achieve this, the tumor sub-regions, including the enhancing tumor, non-enhancing necrotic tumor core, and edema, were segmented for each patient based on the labels available in the BraTS dataset. The Euclidean distance algorithm was utilized to calculate the largest diameter of the enhancing tumor, non-enhancing necrotic tumor core, and edema regions.

3.6 Prediction models

Regression and classification predictive models were utilized to assess the correlation between the

maximum diameters of sub-regions and their survival outcomes, considering the patient's resection status. For the regression models, the maximum diameters of tumor sub-regions were directly fitted to the patients' survival days to predict the exact duration of survival. In contrast, the classification models aimed to classify patients into two main groups based on their survival days: short and medium survival (< 450 days) and extended survival (> 450 days). This approach provided a binary prediction of survival duration for the classification models.

Linear regression (LR), random forest regression (RFR), and support vector regression (SVR) models were employed to examine the univariate impact of maximum diameter features. The LR models indicate the linear relationship between two variables, with one as the explanatory variable and the other as the dependent variable. The RFR involves fitting multiple decision trees on different subsets of the dataset and averaging their predictions. The SVR is a nonparametric method that uses kernel functions to capture complex relationships between the features and the target variable.

For multivariate feature evaluation, the artificial neural network (ANN), random forest classifier (RFC), and k-nearest neighbors (KNN) models were selected. The ANN is designed to capture complex relationships between inputs and target values through interconnected nodes in different layers. The RFC combines the predictions of multiple decision trees to determine the final output. In the KNN algorithm, the new data point is assigned to the category of its closest neighbors based on similarity.

4. Results

In this section, the outcomes of the conducted research will be presented. This will include the results of the feature reductions applied to the extracted radiomic features, followed by the hypothesis testing of the VIF selected features. Furthermore, the robustness of the maximum diameters of tumor sub-regions is presented independently in univariate prediction models and in combination with the pre-selected radiomic features in multivariate prediction models.

4.1 Radiomic feature reduction approaches

First, following the approach described in Soltani [35], we employed a correlation matrix as the initial feature reduction algorithm, resulting in a reduction of radiomic features from 3910 to 1601. Subsequently, the VIF and PCA reduction methods were applied independently to the dataset selected by the correlation matrix. With the VIF selection method, the number of radiomic features was further reduced to 153 from the initial 1601. The PCA algorithm reduced the number of radiomic features from 1601 to 66.

4.2 Hypothesis testing

The Benjamini-Hochberg correction method was employed to select VIF features with the strongest correlation to patients' OS. Three features, namely *T2waveletHLL first order Skewness*, *T1waveletLHH first order Mean*, and *T2.log-sigma-3-0-mm 3D glszm Zone Percentage*, were chosen based on controlling the false discovery rate. These features were utilized in the LR model, and their correlation with OS was presented in **Table 1**. The p-values were calculated to determine the significance of the correlation between the selected VIF features and patients' OS using the linear correlation model. For the NA resection status, the selected features show similar values for MSE, RMSE, and Mean AE. However, the p-value indicates that *T1wavelet-LHH first order Mean* has the highest correlation, with the lowest value of 0.27. On the other hand, within the GTR dataset, *T2wavelet-HLL first order Skewness* feature has the lowest p-value of 0.159, indicating a strong correlation with OS.

4.3 Univariate prediction models

Table 2 presents the results of the regression models. The GTR dataset shows lower errors and better performance compared to the NA dataset. The average mean absolute error (MAE) and root mean squared error (RMSE) for the GTR dataset are 210

and 297, respectively. In contrast, the average MAE and RMSE for NA subjects are 242 and 315.

Spearman's correlation coefficients were also calculated. The majority of the coefficients are negative, indicating a strong correlation between higher tumor maximum diameters and lower survivals. For the GTR dataset, the correlation coefficient is approximately –0.08, while for the NA dataset, it is more decisive, with an average of –0.25. Comparing these results to **Table 1**, it becomes evident that the tumor sub-regions' maximum diameters have a greater impact on patients' OS than the selected VIF features.

The average p-values for sub-regions maximum diameters in the NA dataset are 0.035, significantly lower than the selected VIF features (0.436). Similarly, in the GTR dataset, the average p-values extracted from the linear regression for sub-regions' maximum diameters are 0.425, compared to 0.524 for VIF features. Similarly, MSE, RMSE, and MAE indicate a higher correlation of the newly extracted features compared to the nominated VIF features. The results of the linear regression model are visually depicted in **Figure 3**. **Figures 3a, 3b, and 3c** depict the Spearman correlation between the survival days of GTR patients and their respective non-enhancing tumor diameter, enhancing tumor diameter, and edema diameter. Similarly, **Figures 3d, 3e, and 3f** illustrate the Spearman correlation between the survival days of NA patients and their corresponding non-enhancing tumor diameter, enhancing tumor diameter, and edema diameter. The Spearman correlations, as presented in the subplots of **Figure 3**, along with the p-values from the regression models in **Table 2**, reveal that the diameters of tumor sub-

Table 1. Linear correlation analysis of VIF-selected features with overall survival.

Feature	Spearman R	MSE	RMSE	Mean AE	p value	Spearman R	MSE	RMSE	Mean AE	p value
	NA resection status					GTR resection status				
T2.wavelet HLL_ firstorder_Skewness	0.032	106745	326.71	264.25	0.622	0.129	62771	250.54	187.53	0.159
T1.wavelet-LHH_ firstorder_Mean	–0.109	103049	321.01	257.18	0.270	–0.005	58429	241.72	180.72	0.483
T2.log-sigma-3-0-mm-3D _glszm_ ZonePercentage	0.096	99680	315.72	259.00	0.417	0.128	59422	243.76	182.47	0.932

Table 2. Comparing regression model performance for various resection status types: D1 denotes the non-enhancing necrotic tumor core's diameter, D2 represents the enhancing tumor's diameter, and D3 indicates the edema's diameter.

Feature	Model	Spearman R	MSE	RMSE	Mean AE	p value	Model	Spearman R	MSE	RMSE	Mean AE	p value
	NA resection status						GTR resection status					
D_1	**LR**	–0.276	80414	283.57	232.37	0.012	LR	–0.076	63023	251.04	191.36	0.130
	RFR	–0.037	79671	282.26	221.38	0.278	RFR	0.302	71840	268.03	219.74	0.270
	SVR	0.050	93365	305.55	227.26	0.024	SVR	–0.210	65031	255.01	186.74	0.280
D_2	**LR**	–0.239	83991	289.81	233.59	0.085	LR	–0.085	73858	271.76	199.17	0.644
	RFR	–0.153	96529	310.69	260.66	0.517	RFR	–0.143	177719	421.568	267.20	0.545
	SVR	0.467	93155	305.21	227.24	0.037	SVR	–0.038	65190	255.32	186.88	0.870
D_3	**LR**	–0.248	98139	313.27	268.40	0.010	LR	–0.09	77189	277.83	200.31	0.502
	RFR	–0.056	127703	357.35	290.26	0.813	RFR	–0.157	182101	426.73	263.07	0.507
	SVR	0.416	153822	392.20	221.67	0.068	SVR	–0.20	65289	255.51	186.96	0.390

regions for NA patients exhibit a stronger correlation with survival days (average Spearman correlation of –0.3 and average p-value of 0.035) compared to GTR patients (average Spearman correlation of –0.12 and average p-value of 0.425).

4.4 Multivariate prediction models

To transform the survival outcomes into binary categories, a midpoint of 450 days was selected based on the suggestion from the BraTs challenge (considering long-survivors as those with survival times greater than 450 days and short-survivors as those with survival times less than 450 days). This choice offers an additional advantage since the dataset is already balanced, eliminating the need to address any potential issues related to imbalanced data.

The regression models highlight the effectiveness of tumor sub-regions' maximum diameters. In the classification methods (ANN, RFC, and KNN), the aim was to assess the robustness of the new features when combined with radiomics. The dataset was split into training, validation, and test sets (60% for training, 20% for validation, and 20% for testing). The results of the test set can be found in **Table 3** and **Table 4**.

Across most algorithms, the presence of tumor sub-regions' maximum diameters shows a positive impact on the prediction of OS. The inclusion of the features improved the accuracy and precision of the classification methods by approximately 5%. The highest performance is observed in PCA-selected features for GTR patients, achieving an accuracy of 80%. Furthermore, integrating radiomics with tumor sub-regions' maximum diameters noticeably improved the area under the curve (AUC) values. In the GTR dataset, the combination of VIF-selected features and the maximum diameters of tumor sub-regions achieved the highest AUC of 70%. When the sub-regions' maximum diameters were added to radiomics,

Table 3. Performance comparison of classification models for patients reported as gross total resection status (GTR).

Model	Accuracy	Precision	Sensitivity	Specificity	AUC	Model	Accuracy	Precision	Sensitivity	Specificity	AUC
VIF-based feature subset						**VIF-based feature subset and tumor sub-regions diameter**					
ANN	0.70	0.44	0.81	0.55	0.67	ANN	0.70	0.55	0.81	0.55	0.70
KNN	0.70	0.68	0.70	0.67	0.60	KNN	0.80	0.75	0.82	0.67	0.67
RFC	0.64	0.57	0.81	0.50	0.59	RFC	0.68	0.63	0.87	0.67	0.68
PCA-based feature subset						**PCA-based feature subset and tumor sub-regions diameter**					
ANN	0.65	0.76	0.71	0.50	0.60	ANN	0.69	0.69	0.75	0.50	0.63
KNN	0.60	0.44	0.66	0.71	0.60	KNN	0.75	0.78	0.72	0.78	0.62
RFC	0.64	0.55	0.70	0.40	0.54	RFC	0.64	0.82	0.61	0.42	0.56

Table 4. Performance comparison of classification models for patients reported as unknown resection status (NA).

Model	Accuracy	Precision	Sensitivity	Specificity	AUC	Model	Accuracy	Precision	Sensitivity	Specificity	AUC
VIF-based feature subset						**VIF-based feature subset and tumor sub-regions diameter**					
ANN	0.60	0.71	0.714	0.33	0.56	ANN	0.65	0.40	0.733	0.40	0.58
KNN	0.70	0.63	0.722	1.00	0.55	KNN	0.75	0.82	0.705	1.00	0.69
RFC	0.72	0.63	0.833	0.43	0.64	RFC	0.68	0.72	0.650	0.80	0.65
PCA-based feature subset						**PCA-based feature subset and tumor sub-regions diameter**					
ANN	0.60	0.89	0.533	0.80	0.61	ANN	0.65	0.71	0.769	0.43	0.63
KNN	0.65	0.82	0.631	0.79	0.56	KNN	0.80	0.86	0.737	0.86	0.60
RFC	0.68	0.60	0.695	0.50	0.53	RFC	0.68	0.62	0.714	0.50	0.57

the AUC values for ANN, KNN, and RFC methods increased with an average of 4.42%. Additionally, incorporating the new features led to a nearly 7% increase in AUC for VIF-based features in RFC and KNN methods specifically for the GTR dataset.

It is worth noting that certain algorithms in the study did not show significant improvements when incorporating the newly extracted features. Furthermore, the results did not emphasize the impact of resection status on enhancing survival prediction. These observations can be attributed to the limited dataset size utilized in the study.

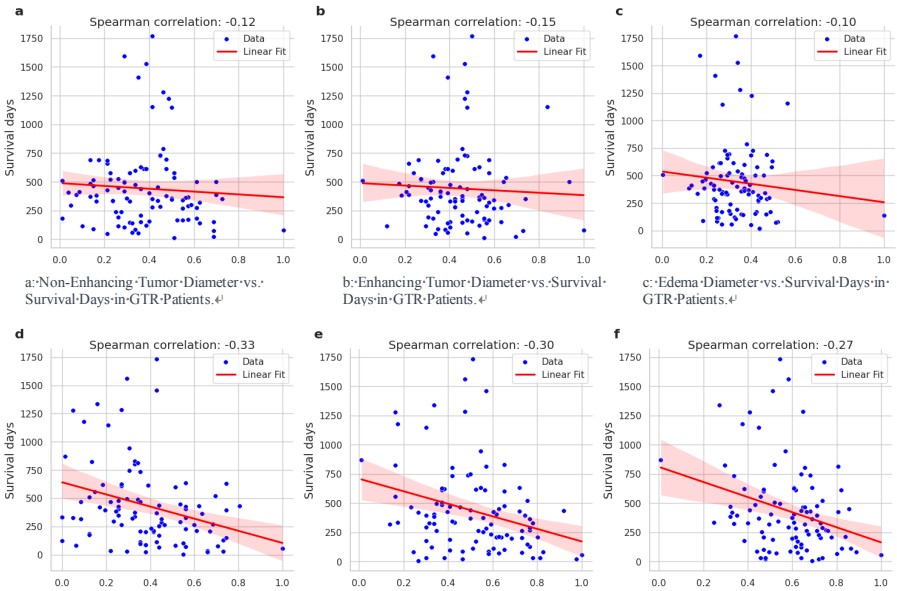

a:·Non-Enhancing·Tumor·Diameter·vs.·Survival·Days·in·GTR·Patients.

b:·Enhancing·Tumor·Diameter·vs.·Survival·Days·in·GTR·Patients.

c:·Edema·Diameter·vs.·Survival·Days·in·GTR·Patients.

Figure·3.d:·Non-Enhancing·Tumor·Diameter·vs.·Survival·Days·in·NA·Patients.

Figure·3.e:·Enhancing·Tumor·Diameter·vs.·Survival·Days·in·NA·Patients.

Figure·3.f:·Edema·Diameter·vs.·Survival·Days·in·NA·Patients.

Figure 3. Scatter plot with linear regression line showing correlation between maximum diameter values (D1: non- enhancing tumor diameter, D2: enhancing tumor diameter, D3: edema diameter) and survival days, stratified by resection status. Graphs a, b, and c represent patients with GTR resection status, while graphs d, e, and f represent patients with NA resection status.

5. Discussion

In recent years, the use of machine learning in medical image analysis has been extensively explored in various studies. Many of these studies have focused on cancer datasets and utilized computer-aided learning algorithms. However, the resection status, which refers to the extent of surgical removal of the tumor, has often been overlooked [9].

In several previous research works, all types of resection status have been combined and used together in the learning algorithms [44–48]. Similarly, radiomics has been employed for quantitative analysis of MRI [49] and 3D deep feature learning [50] without specifically considering the resection status.

In our study, we examined the influence of resection status on regression and classification models. While certain learning algorithms exhibited improved performance when trained on specific resection statuses, the difference was not statistically significant in some cases. These findings suggest that resection status is a potentially important factor in learning algorithms, but a larger and more diverse dataset is required for a more comprehensive evaluation of its impact on survival prediction.

Radiomic features have been extensively employed in quantitative image analysis studies, and numerous research works have investigated their effectiveness. However, the reported accuracies in these studies have been limited. For instance, Sun [51] and Wijethilake [52] utilized radiomics in their image analysis studies but achieved learning accuracies below 70%. Similarly, Baid [53] employed a multi-layer perceptron (MLP) on radiomic features, resulting in an accuracy of 57.1% and a p-value of 0.427. In another study by Shaheen [54], region-specific radiomic features were the focus of their classification models,

and they attained training and test set accuracies of 47.1% and 55.2%, respectively. In a study by Ammari [55], the entire BraTS dataset was used, incorporating all resection statuses in their predictive models. The AUC results for 9, 12, and 15 months were reported as 85%, 74%, and 58%, respectively. Furthermore, Calabrese [56] demonstrated that combining radiomics and deep learning features improves the accuracy of radiogenomic prediction for common glioblastoma genetic biomarkers compared to using either feature alone. In a recent study by Manjunath [57], radiomic features extracted from postcontrast T1-weighted (T1) images using 3D Slicer were employed for machine learning training. Among their evaluated models, the weighted subspace random forest exhibited the highest values for both the AUC and the concordance index (C-index), indicating its superior predictive performance for glioma patient survival. Chiesa [58] conducted a multicentric project, the GLIFA project, to investigate the role of radiomic analysis in guiding radiation target volume delineation for glioblastoma patients who have undergone total or near-total resection. This study aimed to personalize radiation treatment based on radiomic features extracted from the tissue around the resection cavity. The developed radiomic model was able to discriminate between patients with low-risk and high-risk relapse at 6 months with an AUC of 78.5%. Tran [59] focused on the prediction of survival of glioblastoma patients using local spatial relationships and global structure awareness in FLAIR MRI brain images, highlighting the utilization of radiomic features and machine learning models for survival prediction. The accuracy of the model is reported to be 0.621, and the Spearman's Rho is 0.576 in the validation set. Considering these findings, as well as our own study, it becomes evident that radiomic features alone may not be accurate enough for independent clinical applications especially for glioblastoma [60]. The tumor volumes and shape have shown great potential for the patients' OS cancer staging status. Here, we focused on the maximum diameters of tumor sub-regions. In binary OS classification models, the incorporation of additional features alongside radiomics yielded visible effects, suggesting that tumor sub-regions' maximum diameters can enhance the accuracy and improve the performance of the models. The regression models clearly showed the correlation between the maximum diameters of tumor sub-regions and patients' OS. The Benjamini-Hochberg algorithm identified three VIF-selected features that are highly relevant to OS. Notably, the correlation between the maximum diameters of tumor sub-regions and patients' OS is stronger than the correlation observed with the most correlated radiomic features selected using the VIF method. In contrast to Weninger's [9] research, where OS was categorized into three groups, we opted for a binary output in the classification algorithms due to its higher learning rates and accuracies. Adding tumor sub-regions' maximum diameters to radiomics improved the performance of the machine learning algorithms used in this study. This improvement has significant implications for developing better clinical treatment strategies and predicting cancer aggressiveness. To enhance the effectiveness of this approach, utilizing a broader and more diverse dataset is recommended. Therefore, radiomics should be considered an additional quantitative feature for improving the prediction of patients' OS.

Efforts have been made to utilize machine learning and imaging for the diagnosis and classification of cancer [61]. Quantitative imaging offers the potential to extract valuable features that may not be perceptible to clinicians. Therefore, combining essential medical imaging features identified by radiologists with quantitative medical imaging data can enhance the accuracy of evaluating the type and severity of cancer in patients.

Similar to previous studies, the achieved accuracies in both regression and classification models are not notably high, which can be attributed to the limitations of the dataset used. To overcome this issue, it is necessary to employ a larger and more comprehensive dataset, which would help address overfitting problems during training and validation. Moreover, the exploration and identification of novel

imaging features, alongside radiomics, have the potential to enhance the predictive capabilities of OS and improve the precision and accuracy of learning algorithms. This, in turn, can facilitate their practical use in medical treatments.

6. Conclusions

In this study, we utilized the BraTS 2019 training dataset to investigate the relationship between the maximum diameters of tumor sub-regions and patients' OS. The regression models employed in our analysis revealed a clear correlation between the maximum diameters of tumor sub-regions and patients' OS. Additionally, we explored the effectiveness of integrating the newly extracted features with radiomics using classification models. Our findings demonstrated that the inclusion of tumor sub-regions' maximum diameters in the classification models yielded positive responses. This was observed in both the GTR and NA datasets, with an average increase of 4.58% in accuracy. The differences in results between the GTR and NA datasets in some of the machine learning algorithms further highlighted the resection status as a potentially important factor in the prediction models.

This study considered 450 days as the midpoint for survival days, leading to binary classification. However, utilizing a more extensive and diverse dataset with a broader class distribution would enable multiple classifications, providing a more accurate estimation of patients' survival rates and enhancing generalizability. Additionally, assessing additional features related to the medical characteristics of tumor regions would improve the interpretability of machine learning models, ensuring that these features hold tangible medical and clinical significance for validation. The models employed in this study exhibit computational efficiency, underscoring their inherent advantages. As we consider future directions, exploring alternative deep learning models, particularly transformer-based ones, and incorporating additional clinical and genetic data may demand increased computational resources. However, the potential for achieving superior results justifies the computational costs for advancing our understanding and applications in this domain. Also, a deeper investigation into the NA characteristics of resection status is recommended to enhance understanding and enable a robust comparison with GTA resection status.

Author Contributions

RB, AB, and NS preprocessed the data set, performed algorithm implementation, and wrote the manuscript. MS and KR supervised the work, read and edited the manuscript, and discussed the results. All authors contributed to the article and approved the submitted version.

Informed Consent

Ethical review and approval were not required for the study on human participants in accordance with the local legislation and institutional requirements. Written informed consent for participation was not required for this study in accordance with the national legislation and the institutional requirements.

Data Availability

Publicly available datasets were analyzed in this study. This data can be found here: https://www.med.upenn.edu/sbia/brats2018/registration.html.

Conflicts of Interest

The authors declare that the research was conducted in the absence of any commercial or financial relationships that could be construed as a potential conflict of interest.

References

[1] Garanti, T., Alhnan, M.A., Wan, K.W., 2021. The potential of nanotherapeutics to target brain tumors: Current challenges and future opportunities. Nanomedicine. 16(21), 1833–1837. DOI: https://doi.org/10.2217/nnm-2021-0134

[2] Goodenberger, M.L., Jenkins, R.B., 2012. Genetics of adult glioma. Cancer Genetics. 205(12), 613–621.
DOI: https://doi.org/10.1016/j.cancergen.2012.10.009

[3] Atkinson, M., Juhász, C., Shah, J., et al., 2008. Paradoxical imaging findings in cerebral gliomas. Journal of the Neurological Sciences. 269(1–2), 180–183.
DOI: https://doi.org/10.1016/j.jns.2007.12.029

[4] Wang, Y., Zhao, W., Xiao, Z., et al., 2020. A risk signature with four autophagy-related genes for predicting survival of glioblastoma multiforme. Journal of Cellular and Molecular Medicine. 24(7), 3807–3821.
DOI: https://doi.org/10.1111/jcmm.14938

[5] Holland, E.C., 2000. Glioblastoma multiforme: The terminator. Proceedings of the National Academy of Sciences. 97(12), 6242–6244.
DOI: https://doi.org/10.1073/pnas.97.12.6242

[6] Gomez, S.L., Shariff-Marco, S., DeRouen, M., et al., 2015. The impact of neighborhood social and built environment factors across the cancer continuum: Current research, methodological considerations, and future directions. Cancer. 121(14), 2314–2330.
DOI: https://doi.org/10.1002/cncr.29345

[7] McTiernan, A., Friedenreich, C.M., Katzmarzyk, P.T., et al., 2019. Physical activity in cancer prevention and survival: A systematic review. Medicine and Science in Sports and Exercise. 51(6), 1252–1261.
DOI: https://doi.org/10.1249/MSS.0000000000001937

[8] Carrera, P.M., Kantarjian, H.M., Blinder, V.S., 2018. The financial burden and distress of patients with cancer: Understanding and stepping-up action on the financial toxicity of cancer treatment. CA: A Cancer Journal for Clinicians. 68(2), 153–165.
DOI: https://doi.org/10.3322/caac.21443

[9] Weninger, L., Haarburger, C., Merhof, D., 2019. Robustness of radiomics for survival prediction of brain tumor patients depending on resection status. Frontiers in Computational Neuroscience. 13, 73.
DOI: https://doi.org/10.3389/fncom.2019.00073

[10] Jonklaas, J., Nogueras-Gonzalez, G., Munsell, M., et al., 2012. The impact of age and gender on papillary thyroid cancer survival. The Journal of Clinical Endocrinology & Metabolism. 97(6), E878–E887.
DOI: https://doi.org/10.1210/jc.2011-2864

[11] Chowdhary, C.L., Acharjya, D.P., 2020. Segmentation and feature extraction in medical imaging: A systematic review. Procedia Computer Science. 167, 26–36.
DOI: https://doi.org/10.1016/j.procs.2020.03.179

[12] Choi, Y., Nam, Y., Jang, J., et al., 2021. Radiomics may increase the prognostic value for survival in glioblastoma patients when combined with conventional clinical and genetic prognostic models. European Radiology. 31, 2084–2093.
DOI: https://doi.org/10.1007/s00330-020-07335-1

[13] Ardakani, A.A., Bureau, N.J., Ciaccio, E.J., et al., 2022. Interpretation of radiomics features—a pictorial review. Computer Methods and Programs in Biomedicine. 215, 106609.
DOI: https://doi.org/10.1016/j.cmpb.2021.106609

[14] Tomaszewski, M.R., Gillies, R.J., 2021. The biological meaning of radiomic features. Radiology. 298(3), 505–516.
DOI: https://doi.org/10.1148/radiol.2021202553

[15] Hooper, G.W., Ginat, D.T., 2023. MRI radiomics and potential applications to glioblastoma. Frontiers in Oncology. 13, 1134109.
DOI: https://doi.org/10.3389/fonc.2023.1134109

[16] Zhu, J., Ye, J., Dong, L., et al., 2023. Non-invasive prediction of overall survival time for glioblastoma multiforme patients based on multimodal MRI radiomics. International Journal of Imaging Systems and Technology. 33(4), 1261–1274.
DOI: https://doi.org/10.1002/ima.22869

[17] Li, Y., Bao, L., Yang, C., et al., 2023. A multi-

parameter radiomic model for accurate prognostic prediction of glioma. MedComm–Future Medicine. 2(2), e41.
DOI: https://doi.org/10.1002/mef2.41

[18] Shboul, Z.A., Vidyaratne, L., Alam, M., et al., 2018. Glioblastoma and survival prediction. Brainlesion: Glioma, multiple sclerosis, stroke and traumatic brain injuries. Springer International Publishing: Cham. pp. 358–368.
DOI: https://doi.org/10.1007/978-3-319-75238-9_31

[19] Feng, X., Tustison, N.J., Patel, S.H., et al., 2020. Brain tumor segmentation using an ensemble of 3d u-nets and overall survival prediction using radiomic features. Frontiers in Computational Neuroscience. 14, 25.
DOI: https://doi.org/10.3389/fncom.2020.00025

[20] Bakas, S., Reyes, M., Jakab, A., et al., 2018. Identifying the best machine learning algorithms for brain tumor segmentation, progression assessment, and overall survival prediction in the BRATS challenge. arXiv preprint arXiv:1811.02629.

[21] Baid, U., Talbar, S., Rane, S., et al., 2019. Deep learning radiomics algorithm for gliomas (drag) model: A novel approach using 3d unet based deep convolutional neural network for predicting survival in gliomas. Brainlesion: Glioma, multiple sclerosis, stroke and traumatic brain injuries. Springer International Publishing: Cham. pp. 369–379.
DOI: https://doi.org/10.1007/978-3-030-11726-9_33

[22] Jungo, A., McKinley, R., Meier, R., et al., 2018. Towards uncertainty-assisted brain tumor segmentation and survival prediction. Brainlesion: Glioma, multiple sclerosis, stroke and traumatic brain injuries. Springer International Publishing: Cham. pp. 474–485.
DOI: https://doi.org/10.1007/978-3-319-75238-9_40

[23] Puybareau, E., Tochon, G., Chazalon, J., et al., 2019. Segmentation of gliomas and prediction of patient overall survival: A simple and fast procedure. Brainlesion: Glioma, multiple sclerosis, stroke and traumatic brain injuries. Springer International Publishing: Cham. pp. 199–209.
DOI: https://doi.org/10.1007/978-3-030-11726-9_18

[24] Sun, L., Zhang, S., Luo, L., 2019. Tumor segmentation and survival prediction in glioma with deep learning. Brainlesion: Glioma, multiple sclerosis, stroke and traumatic brain injuries. Springer International Publishing: Cham. pp. 83–93.
DOI: https://doi.org/10.1007/978-3-030-11726-9_8

[25] Choi, Y.S., Ahn, S.S., Chang, J.H., et al., 2020. Machine learning and radiomic phenotyping of lower grade gliomas: Improving survival prediction. European Radiology. 30, 3834–3842.
DOI: https://doi.org/10.1007/s00330-020-06737-5

[26] Wankhede, D.S., Selvarani, R., 2022. Dynamic architecture based deep learning approach for glioblastoma brain tumor survival prediction. Neuroscience Informatics. 2(4), 100062.
DOI: https://doi.org/10.1016/j.neuri.2022.100062

[27] Hu, Z., Yang, Z., Zhang, H., et al., 2022. A deep learning model with radiomics analysis integration for glioblastoma post-resection survival prediction. arXiv preprint arXiv:2203.05891.

[28] Fang, L., Wang, X., 2022. Brain tumor segmentation based on the dual-path network of multi-modal MRI images. Pattern Recognition. 124, 108434.
DOI: https://doi.org/10.1016/j.patcog.2021.108434

[29] Liu, J., Li, M., Wang, J., et al., 2014. A survey of MRI-based brain tumor segmentation methods. Tsinghua Science and Technology. 19(6), 578–595.
DOI: https://doi.org/10.1109/TST.2014.6961028

[30] Senders, J.T., Staples, P., Mehrtash, A., et al.,

2020. An online calculator for the prediction of survival in glioblastoma patients using classical statistics and machine learning. Neurosurgery. 86(2), E184–E192.
DOI: https://doi.org/10.1093/neuros/nyz403

[31] Menze, B.H., Jakab, A., Bauer, S., et al., 2014. The multimodal brain tumor image segmentation benchmark (BRATS). IEEE Transactions on Medical Imaging. 34(10), 1993–2024.
DOI: https://doi.org/10.1109/TMI.2014.2377694

[32] Bakas, S., Akbari, H., Sotiras, A., et al., 2017. Advancing the cancer genome atlas glioma MRI collections with expert segmentation labels and radiomic features. Scientific Data. 4, 170117.
DOI: https://doi.org/10.1038/sdata.2017.117

[33] Segmentation Labels for the Pre-operative Scans of the TCGA-GBM Collection [Internet]. The Cancer Imaging Archive. Available from: https://doi.org/10.7937/K9/TCIA.2017.KLXWJJ1Q

[34] Segmentation Labels and Radiomic Features for the Pre-operative Scans of the TCGA-LGG Collection [Internet]. The Cancer Imaging Archive. Available from: https://doi.org/10.7937/K9/TCIA.2017.GJQ7R0EF

[35] Soltani, M., Bonakdar, A., Shakourifar, N., et al., 2021. Efficacy of location-based features for survival prediction of patients with glioblastoma depending on resection status. Frontiers in Oncology. 11, 661123.
DOI: https://doi.org/10.3389/fonc.2021.661123

[36] Tustison, N.J., Avants, B.B., Cook, P.A., et al., 2010. N4ITK: Improved N3 bias correction. IEEE Transactions on Medical Imaging. 29(6), 1310–1320.
DOI: https://doi.org/10.1109/TMI.2010.2046908

[37] Gaillochet, M., Tezcan, K.C., Konukoglu, E., 2020. Joint reconstruction and bias field correction for undersampled MR imaging. Medical image computing and computer-assisted intervention. Springer International Publishing: Cham. pp. 44–52.
DOI: https://doi.org/10.1007/978-3-030-59713-9_5

[38] Van Griethuysen, J.J., Fedorov, A., Parmar, C., et al., 2017. Computational radiomics system to decode the radiographic phenotype. Cancer Research. 77(21), e104–e107.
DOI: https://doi.org/10.1158/0008-5472.CAN-17-0339

[39] Bzdok, D., 2017. Classical statistics and statistical learning in imaging neuroscience. Frontiers in Neuroscience. 11, 543.
DOI: https://doi.org/10.3389/fnins.2017.00543

[40] Gillies, R.J., Kinahan, P.E., Hricak, H., 2016. Radiomics: Images are more than pictures, they are data. Radiology. 278(2), 563–577.
DOI: https://doi.org/10.1148/radiol.2015151169

[41] Abdi, H., Williams, L.J., 2010. Principal component analysis. Wiley Interdisciplinary Reviews: Computational Statistics. 2(4), 433–459.
DOI: http://dx.doi.org/10.1002/wics.101

[42] Kambhatla, N., Leen, T.K., 1997. Dimension reduction by local principal component analysis. Neural Computation. 9(7), 1493–1516.
DOI: https://doi.org/10.1162/neco.1997.9.7.1493

[43] Benjamini, Y., Hochberg, Y., 1995. Controlling the false discovery rate: A practical and powerful approach to multiple testing. Journal of the Royal Statistical Society: Series B (Methodological). 57(1), 289–300.
DOI: https://doi.org/10.1111/j.2517-6161.1995.tb02031.x

[44] Gutman, D.A., Cooper, L.A., Hwang, S.N., et al., 2013. MR imaging predictors of molecular profile and survival: Multi-institutional study of the TCGA glioblastoma data set. Radiology. 267(2), 560–569.
DOI: https://doi.org/10.1148/radiol.13120118

[45] Macyszyn, L., Akbari, H., Pisapia, J.M., et al., 2015. Imaging patterns predict patient survival and molecular subtype in glioblastoma via machine learning techniques. Neuro-oncology. 18(3), 417–425.
DOI: https://doi.org/10.1093/neuonc/nov127

[46] Kickingereder, P., Burth, S., Wick, A., et al., 2016. Radiomic profiling of glioblastoma:

Identifying an imaging predictor of patient survival with improved performance over established clinical and radiologic risk models. Radiology. 280(3), 880–889.
DOI: https://doi.org/10.1148/radiol.2016160845

[47] Lao, J., Chen, Y., Li, Z.C., et al., 2017. A deep learning-based radiomics model for prediction of survival in glioblastoma multiforme. Scientific Reports. 7, 10353.
DOI: https://doi.org/10.1038/s41598-017-10649-8

[48] Li, Q., Bai, H., Chen, Y., et al., 2017. A fully-automatic multiparametric radiomics model: towards reproducible and prognostic imaging signature for prediction of overall survival in glioblastoma multiforme. Scientific Reports. 7, 14331.
DOI: https://doi.org/10.1038/s41598-017-14753-7

[49] Zhang, Z., Jiang, H., Chen, X., et al., 2014. Identifying the survival subtypes of glioblastoma by quantitative volumetric analysis of MRI. Journal of Neuro-oncology. 119, 207–214.
DOI: https://doi.org/10.1007/s11060-014-1478-2

[50] Nie, D., Zhang, H., Adeli, E., et al., 2016. 3D deep learning for multi-modal imaging-guided survival time prediction of brain tumor patients. Medical image computing and computer-assisted intervention. Springer International Publishing: Cham. pp. 212–220.
DOI: https://doi.org/10.1007/978-3-319-46723-8_25

[51] Sun, W., Jiang, M., Dang, J., et al., 2018. Effect of machine learning methods on predicting NSCLC overall survival time based on Radiomics analysis. Radiation Oncology. 13, 197.
DOI: https://doi.org/10.1186/s13014-018-1140-9

[52] Wijethilake, N., Islam, M., Ren, H., 2020. Radiogenomics model for overall survival prediction of glioblastoma. Medical & Biological Engineering & Computing. 58, 1767–1777.
DOI: https://doi.org/10.1007/s11517-020-02179-9

[53] Baid, U., Rane, S.U., Talbar, S., et al., 2020. Overall survival prediction in glioblastoma with radiomic features using machine learning. Frontiers in Computational Neuroscience. 14, 61.
DOI: https://doi.org/10.3389/fncom.2020.00061

[54] Shaheen, A., Burigat, S., Bagci, U., et al., 2020. Overall survival prediction in gliomas using region-specific radiomic features. Machine learning in clinical neuroimaging and radiogenomics in neuro-oncology. Springer International Publishing: Cham. pp. 259–267.
DOI: https://doi.org/10.1007/978-3-030-66843-3_25

[55] Ammari, S., Sallé de Chou, R., Balleyguier, C., et al., 2021. A predictive clinical-radiomics nomogram for survival prediction of glioblastoma using MRI. Diagnostics. 11(11), 2043.
DOI: https://doi.org/10.3390/diagnostics11112043

[56] Calabrese, E., Rudie, J.D., Rauschecker, A.M., et al., 2022. Combining radiomics and deep convolutional neural network features from preoperative MRI for predicting clinically relevant genetic biomarkers in glioblastoma. Neuro-Oncology Advances. 4(1), vdac060.
DOI: https://doi.org/10.1093/noajnl/vdac060

[57] Manjunath, M., Saravanakumar, S., Kiran, S., et al., 2023. A comparison of machine learning models for survival prediction of patients with glioma using radiomic features from MRI scans. Indian Journal of Radiology and Imaging. 33(3), 338–343.
DOI: https://doi.org/10.1055/s-0043-1767786

[58] Chiesa, S., Russo, R., Beghella Bartoli, F., et al., 2023. MRI-derived radiomics to guide post-operative management of glioblastoma: Implication for personalized radiation treatment volume delineation. Frontiers in Medicine. 10, 1059712.
DOI: https://doi.org/10.3389/fmed.2023.1059712

[59] Tran, M.T., Yang, H.J., Kim, S.H., et al., 2023. Prediction of survival of glioblastoma patients using local spatial relationships and global

structure awareness in FLAIR MRI brain images. IEEE Access. 11, 37437–37449. DOI: https://doi.org/10.1109/ACCESS.2023.3266771

[60] Martin, P., Holloway, L., Metcalfe, P., et al., 2022. Challenges in glioblastoma radiomics and the path to clinical implementation. Cancers. 14(16), 3897. DOI: https://doi.org/10.3390/cancers14163897

[61] Khan, M.A., Ashraf, I., Alhaisoni, M., et al., 2020. Multimodal brain tumor classification using deep learning and robust feature selection: A machine learning application for radiologists. Diagnostics. 10(8), 565. DOI: https://doi.org/10.3390/diagnostics10080565